Hydrogeol J (2017) 25:575–588
DOI 10.1007/s10040-016-1507-7

REPORT

Characterizing the interaction of groundwater and surface water in the karst aquifer of Fangshan, Beijing (China)

Haibo Chu[1] · **Jiahua Wei**[1,2] · **Rong Wang**[3] · **Baodong Xin**[3]

Received: 7 May 2016 / Accepted: 22 November 2016 / Published online: 14 December 2016

Abstract Correct understanding of groundwater/surface-water (GW–SW) interaction in karst systems is of greatest importance for managing the water resources. A typical karst region, Fangshan in northern China, was selected as a case study. Groundwater levels and hydrochemistry analyses, together with isotope data based on hydrogeological field investigations, were used to assess the GW–SW interaction. Chemistry data reveal that water type and the concentration of cations in the groundwater are consistent with those of the surface water. Stable isotope ratios of all samples are close to the local meteoric water line, and the ^{3}H concentrations of surface water and groundwater samples are close to that of rainfall, so isotopes also confirm that karst groundwater is recharged by rainfall. Cross-correlation analysis reveals that rainfall leads to a rise in groundwater level with a lag time of 2 months and groundwater exploitation leads to a fall within 1 month. Spectral analysis also reveals that groundwater level, groundwater exploitation and rainfall have significantly similar response periods, indicating their possible inter-relationship. Furthermore, a multiple nonlinear regression model indicates that groundwater level can be negatively correlated with groundwater exploitation, and positively correlated with rainfall. The overall results revealed that groundwater level has a close correlation with groundwater exploitation and rainfall, and they are indicative of a close hydraulic connection and interaction between surface water and groundwater in this karst system.

Keywords Groundwater/surface-water relations · Hydrochemistry · Groundwater level · Isotope · China

✉ Jiahua Wei
weijiahua@tsinghua.edu.cn

[1] State Key Laboratory of Hydroscience & Engineering, Tsinghua University, Beijing 100084, China

[2] State Key Laboratory of Plateau Ecology and Agriculture, Sanjiangyuan Collaborative Innovation Center, Qinghai University, Xining 810016, China

[3] Beijing Institute of Hydrogeology and Engineering Geology, Beijing 100195, China

Introduction

Karst systems are characteristically challenging hydrogeological environments, involving transmissive fractures and conduits, where continual groundwater/surface-water (GW–SW) interaction has complex and unique characteristics (Gill et al. 2013; Doglioni and Simeone 2014; Eris and Wittenberg 2015). Groundwater and surface water are inseparable components in the hydrological cycle, with one transforming to the other (Banks et al. 2009; Sun et al. 2013). In many previous studies, groundwater and surface water have been treated as independent parts; when building the groundwater simulation model, surface water will be just generalized as the upper boundary, and when building the surface-water simulation model, groundwater will be generalized as the lower boundary (Schmidt et al. 2014; Rugel et al. 2016). This simplification will undoubtedly lose some important information, and thus will not fully reflect the physical processes of the water cycle (Dafny et al. 2010; Charlier et al. 2012; Green et al. 2014). Identification of the processes involved in GW–SW interaction can provide a reliable basis to build an integrated model of the surface water and groundwater. What's more, a correct understanding of the GW–SW interaction can contribute to effective water resources management, identification of the contaminant pathways, and improvement of the ecological environment; however, due to the complex

hydraulic interconnections of fractures and solution openings, it is particularly difficult to characterize GW–SW interaction in karst systems.

Many approaches to characterizing GW–SW interaction have been studied (Table 1). Numerical simulation is an effective method for identifying GW–SW interaction. Scibek et al. (2007) used a three-dimensional (3D) transient groundwater flow model to simulate three climate-related time periods for estimating future impacts of climate change on GW–SW interactions and groundwater levels in Columbia, Canada. Brunner et al. (2010) examined the simulation accuracy of GW–SW interaction with HydroGeoSphere, whereas Ward et al. (2010) coupled near-surface electrical resistivity with conservative solute tracer transport to predict space and time dynamics in solute exchange between the river channel and hyporheic zone; however, numerical modelling requires good conceptual understanding by field investigation. Field investigation is the most basic approach, and the main ways include pumping tests, groundwater velocity monitoring, direct measurements of water flux and so on. Devito et al. (1996) conducted field investigations to study GW–SW interaction with detailed measurements of stream discharge at the upstream and downstream end of their study area, while Oxtobee and Novakowski (2002) had an understanding of GW–SW interaction via field and desk-based investigations in a fractured bedrock environment, including air-photo interpretation, detailed stream surveys, electrical conductivity measurements, and point measurements of hydraulic head and discharge. Hydrochemical analysis, isotope analysis and water level fluctuations were also effective approaches for the understanding of GW–SW interaction (Owor et al. 2011; Yang et al. 2014b). Rodgers et al. (2004) used numerous geochemical and isotopic tracers to study interactions between groundwater and surface water, and the results showed that shallow groundwater flow systems at the edge of a braided floodplain are recharged by effluent streams and hillslope drainage. Kumar et al. (2009) identified the extent of GW–SW interaction processes in an urban setting by major ion chemistry and multivariate statistical techniques. Menning et al. (2015) proves that the interactions between inland hydrological conditions and sea level govern the karst estuary system, via water samples analysis, partial correlation analyses and an isotopic/trace element mass balance tracer method, with the data of short-term tidal fluctuations, long-term rainfall patterns, aquifer groundwater levels, spring discharge, and multiple geochemical parameters. Martinez et al. (2015) identified GW–SW connectivity in headwater catchments of southeast Queensland, Australia, combining long-term hydrochemical data, hydraulic water level data and isotope hydrology. There are also other methods, such as the heat tracer approach, which utilises the difference in temperature between groundwater and surface water to delineate groundwater discharge or recharge zones; and the mass balance approach, which studies GW–SW interactions whereby any change in the properties of surface water can be related to the water sources, so the groundwater component can be identified and quantified (Kalbus et al. 2006; Yao et al. 2015). In this report, hydrochemical analysis, isotope analysis and water level fluctuations were integrated with several statistical methods to more comprehensively and completely identify the hydraulic relationships between surface water and groundwater in the study area.

Many research works about the groundwater and surface water have been carried out in Beijing, China. Zhan et al. (2012) used a hydrological modelling approach to quantify the impact of human activities and climate variability on streamflow using data from 1986 to 1998 in Beijing. Xu et al. (2012a) calculated and analyzed the status of overexploitation of groundwater in the Fangshan plain of Beijing, the results of which showed that the Fangshan plain was seriously

Table 1 A review of the approaches used to characterize GW–SW interaction

Approach	Measures	Study area	Case study
Numerical simulation	A 3D transient groundwater flow model	Columbia, Canada	Scibek et al. (2007)
	HydroGeoSphere	Australia	Brunner et al. (2010)
	A fully coupled finite-element model	Hypothesized examples	Ward et al. (2010)
Field investigation	Pumping tests, groundwater velocity, monitoring, direct measurements of water flux	Canada	Devito et al. (1996)
	Air-photo interpretation, detailed stream surveys, electrical conductivity, point measurements of hydraulic head and discharge	Niagara Peninsula, Canada	Oxtobee and Novakowski (2002)
Hydrochemicalanalysis	Piper diagram, principle component analysis, cluster analysis	Delhi, India	Kumar et al. (2009)
Isotope analysis	Numerous geochemical and isotopic tracers	Cairngorms, Scotland (UK)	Rodgers et al. (2004)
Water level fluctuations	Isotopic/trace element mass, groundwater levels, and spring discharge analysis	Florida, USA	Menning et al. (2015)
	Hierarchical cluster analysis, conceptual model	Southeast Queensland, Australia	Martinez et al. (2015)

over-exploited. Yang et al. (2014a) applied the European Model to assess karst groundwater vulnerability in Fangshan, Beijing, and modified the precipitation regime (P factor) and the concentration of flow (C factor) to adapt to the specificity of the karst; the results indicated that high vulnerability exists near karst caves. The European model provides a simple, yet sound, conceptual framework for vulnerability assessment and mapping for karst hydrogeological environments (Daly et al. 2002). Wei et al. (2015) analyzed the distribution of springs, evaluated the quantity of groundwater resources in the karst aquifer, and developed the model with three exploitation scenarios considering the spring discharge protection; however, little research has been conducted on the interaction of groundwater and surface water.

Understanding and analysis of the interactive relationship between surface water and groundwater in karst regions, are of important theoretical and practical significance for evaluation, development and use of karst water resources (Naughton et al. 2012; Jukić and Denić-Jukić 2015; Zeng et al. 2015). In this report, a typical karst region in northern China was selected as case study, and it is one of most typical carbonated karst regions in the semi-arid area of northern China, where water resources supply–demand issues are very prominent. It is an important water source for the city of Beijing to ensure the stability of water supply and relieve the supply–demand constrictions. This study comprised firstly a brief introduction to the study area and collation of previous research about field investigation surveys, and relevant data were collected. Subsequently the main characteristics of geology and hydrogeology typical of the karst region were further analyzed. The interaction of groundwater and surface water was considered by studying the recharge sources and the flow paths, through groundwater level measurement, hydrochemistry analysis, and isotope data analysis based on the hydrogeological field investigations.

Study area and data

The study area is located in southwestern Beijing, China, known as the site of Peking Man at Zhoukoudian and Fangshan Global Geopark. It is one of most typical karst regions, and karst landforms and karst springs form an important part of the Fangshan landscape. It covers an area of approximately 600 km^2 between 115°30′–115°55′E and 39°30′–39°50′N, within the watershed of the Juma River (Sun et al. 2014; Wang et al. 2015).

Annual rainfall has varied from the maximum value of 1,037.5 mm in 1959 to minimum value 700 mm in 1965. The annual rainfall in the mountains is between 700 and 760 mm, which is about 40 mm higher than that of the plain region. Approximately 95% of the rainfall occurs between April and October. Estimates of evapotranspiration suggest an average of about 579 mm/year, and the annual average temperature ranges from −5.4 to 4.1 °C, with July being the warmest month and January the coldest (Xu et al. 2012b; Zhang et al. 2014). Juma River flows through the study area from north to south with an average flow of about 1.60 m^3/s during 2003–2014.

Field investigations began in the mid-20th century. Hydrogeological maps and geological maps were developed successively with different scales of 1:100,000, 1:50,000, and 1:25,000 (BGMRBM 1991; Wei 2008). In the 1970s, karst water resources investigations were conducted in order to develop water sources. By the 2000s, karst spring discharge and groundwater were continuously monitored in Fangshan. In 2001, karst groundwater samples were analyzed for isotope and water chemistry. A series of geophysical prospecting tests, pumping tests, and dynamic observation and water chemistry and isotope sampling analyses were also carried out successively from 2000 to 2014. The analysis of geological and hydrogeological conditions basically established the formation and structure of Fangshan, and formed a preliminary understanding of the groundwater recharge, flow and discharge conditions. A water supply project which exploits karst groundwater has been in action since 2006 to guarantee water supply for Beijing. Daily pumping data and groundwater level data have been obtained. There are two stream gauging stations named Duya and Zhangfang that have served as control stations on Juma River in this area. The precipitation data from four stations (named Shidu, Puwa, Xiayunling and Nanjiao) in the study area for the last 40 years have been used to analyse the variability of the precipitation and its relationship with groundwater level and exploitation.

Between 2006 and 2012, 52 water-quality samples were collected from the area of Fangshan for hydrochemical analysis: 4 from the Quaternary aquifer, 13 from surface water, and 35 from springs (karst groundwater). The sampling locations, shown in Fig. 1, correspond with some of the most representative springs of the Fangshan area. Water samples were collected and analyzed for pH, total dissolved solids (TDS), Cl^-, SO_4^{2-}, HCO_3^-, Na^+, Ca^{2+} and Mg^{2+}. Additionally, the isotope ratios of $\delta^{18}O$ and δ^2H were analyzed using a Finnegan MAT252 mass spectrometer. Data on the main springs discharge, monthly rainfall and groundwater level were collected from January 2004 to December 2014. These data, and the amount of groundwater exploited from December 2006 to December 2014, are shown in Table 2.

Geology and hydrogeology of the study area

Geology

Geologically the study area is mainly composed of sedimentary and metamorphic rocks (Fig. 1). From old to new, the strata include Changcheng System (Ch), Jixianian System, Qingbaikouan System (Qn), Cambrian system (∈),

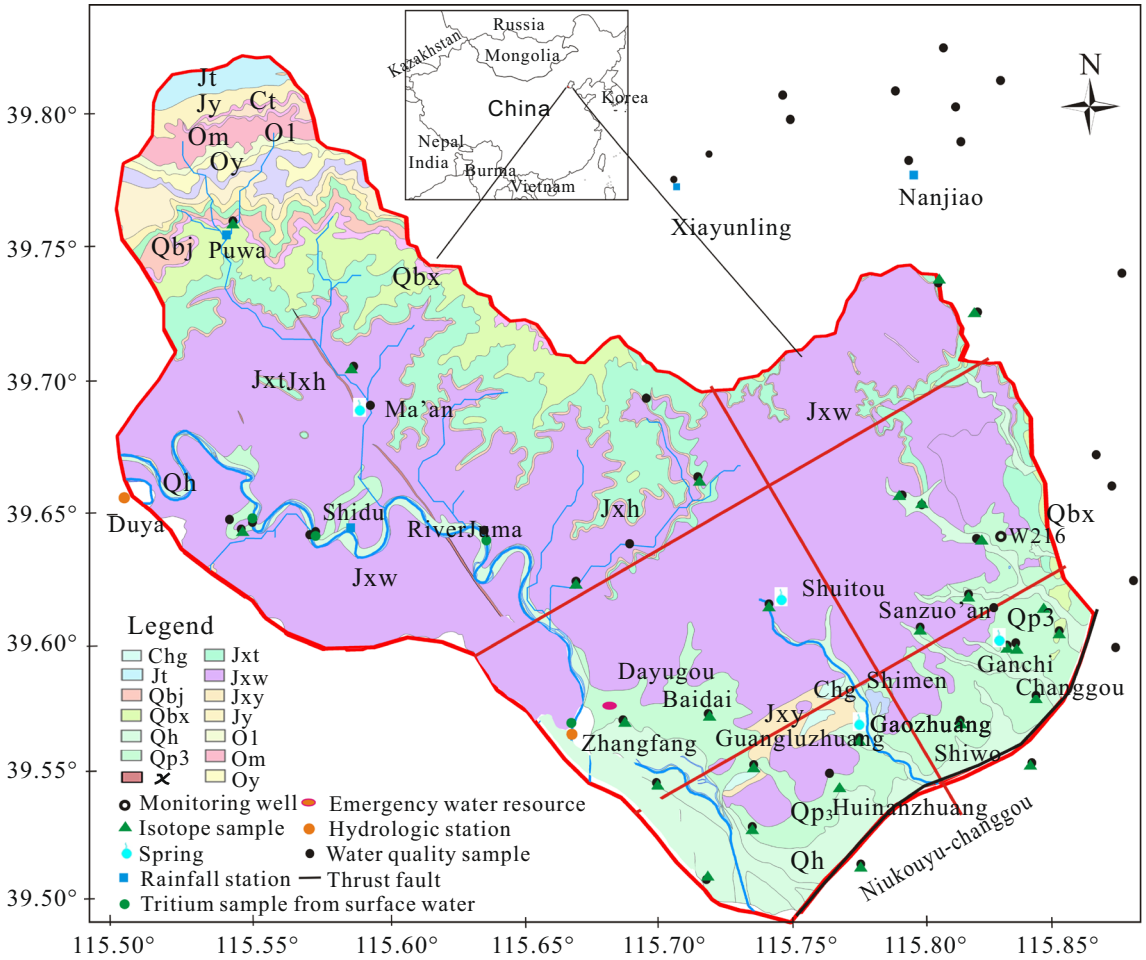

Fig. 1 Hydrogeological map of Fangshan, China

Ordovician system (O), Carboniferous System (C), Permian System (P), Jurassic System (J), Cretaceous system (K), and Quaternary (Q) (Table 3). The Changcheng (Ch) system is only distributed in the east of the study area, where the lithology is quartz sandstone and siliceous dolomite. Quaternary deposits are scarcely distributed in the southeastern hills, valley, and piedmont plain. The Quaternary distribution area is small, with a thickness of less than 20 m; the upper strata are clay and sand, and the lithology of the lower strata is gravel.

Quaternary deposits are zoned, as the lithology changes from the piedmont to the plain. It consists of gravelly sand and loam sand in the piedmont zone, and it consists of gravelly sand, loam sand, occasionally with discontinuous impermeable thin layers of clay, and silty clay in the transition zone; thus it consists of gravel in the plain (Figs. 1 and 2).

Wumishan group (Jxw) dolomite is exposed in the whole area on a large scale. It outcrops widely in the mountain region, and is overlain by Quaternary in the area between the piedmont zone and the plain, and is also overlain by Carboniferous (C)-Permian (P) and Jurassic (J) strata to the southeast of Niukouyu-Changgou thrust fault. In the surrounding village of Shimen, contact metamorphism has occurred, explaining the mineral composition and structure of limestone near the contact zone, and forms the crystalline limestone. There is a distinct channel for groundwater migration, which crosses a set of NE 60–80° fractures and a set of NW 10–25° fractures.

Beiling syncline, Dashihe anticline and Xiayunling-Longmentai synclinorium are shown in Fig. 3. Beiling syncline is located in the east of the study area. The core stratum is comprised of Jurassic, forming the high mountain, and around the edge of Beiling syncline Jurassic strata are followed by Permian and Carboniferous, Ordovician and Cambrian. There are magmatic rocks on the eastern side of the syncline, and Beiling syncline formed the shape of a "crescent moon" due to its compression. Dashihe anticline is located in the north of the study area. The core stratum is comprised of Wumishan (Jxw) in the west and Qingbaikou system (Qn) in the east, and Hongshuizhuang (Jxh) and Tieling (Jxt) strata lies around the edge of Dashihe anticline. The core of the anticline was cut by a river, forming a deep valley. Xiayunling-Longmentai synclinorium is located in the west of the study area; the core stratum is comprised of Tieling (Jxt), Qingbaikou system (Qn), and Cambrian (∈), and Wumishan (Jxw) lies around

Table 2 Summary of sampling, exploitation and other data information

	Parameter	Location	Observation period (year.month)	Sampling interval	Other information
1	Water quality	Sample points shown in Fig. 1	2006.1–2012.12	Twice (in 2006 and 2012)	pH 6.7–8.4, TDS 100–500 mg/L Cl^- 3–38 mg/L, SO_4^{2-} 25–70 mg/L, HCO_3^- 150–350 mg/L, Na^+ 5.5–8.5 mg/L, Ca^{2+} 35–75 mg/L, Mg^{2+} 20–35 mg/L
2	Isotopes	Sample points shown in Fig. 1	2012.6–2012.12	Twice (in 2006 and 2012)	$\delta^{18}O$ −11 to −8‰, δ^2H −70 to −60‰, ^3H 3.2 to 26.3 TU
3	Groundwater level	Zhangfang village W216	2004.1–2014.12	1 month	80–200 m
4	Spring discharge	Ma'an spring, Gaozhuang spring, Shuitou spring, Ganchi spring	2004.1–2014.12	1 month	$0–1 \times 10^4$ m^3/day, $0–7 \times 10^4$ m^3/day, $0–6 \times 10^3$ m^3/day, $0–3 \times 10^4$ m^3/day
5	Rainfall	Xiayunling station, Shidu station, Puwa station, Nanjiao station, Zhangfang station	2004.1–2014.12	1 month	0–400 mm/month
6	Groundwater exploitation	Zhangfang water source	2006.12–2014.12	1 month	$10–500 \times 10^4$ m^3/month
7	Streamflow	Duya and Zhangfang station	2004.1–2014.12	1 month	0–30 m^3/s

the edge of the synclinorium. In addition, there is a special anticline named Sanzuo'an anticline, and it is developed only in the Wumishan (Jxw) group at the center of the village of Sanzuo'an.The faults in the study area are mainly grouped into northeast (NE) and northwest (NW) trending fractures. Niukouyu-Changgou fracture is located in the southeast of the study area, with fault strike of NE30°, as the reverse fault.

Hydrogeology

The aquifer system in this region is formed from Quaternary (Q_{P3}) deposits and dolomite with a total thickness of about 300–500 m. The aquifer system consists of three layers: firstly, the Quaternary aquifer, which plays an important role in receiving and passing downward precipitation recharge. The second layer is the karst aquifer with dissolutionally developed fractures, in which the aquifer medium is nonporous but contains fractures and joints which function as groundwater conduits. The third layer has limited dissolutional development of fractures and is an aquitard. In more detail:

The Quaternary aquifer, the *first layer*, has a thickness of 10–20 m, and the exploitation potential for water supply is limited. The hydraulic conductivity (K) of the aquifer is 0.5–20 m/day and well productivity is in the range 500–1,000 m^3/day.

The *second layer* consists of Wumishan group (Jxw) dolomite, which is the main layer to supply water in the study area. The water-rich area can be divided into four zones:

1. Near the contact zone between the limestone of Wumishan group (Jxw) and the impermeable shale. Ganchi spring is caused by karst groundwater encountering the impermeable shale, and the outflow reaches 19,008–24,192 m^3/day. Here also, Gaozhuang spring is the ascending spring formed where karst groundwater encounters granite and overflows to the surface through the thin Quaternary layer; the spring discharge reaches $4.0–6 \times 10^4$ m^3/day
2. Near all the fracture zones well productivity is about 2,400 m^3/day
3. Near the area where the horizontal layer transitions sharply into a vertical layer
4. Near the distribution of Wumishan group (Jxw) dolomite

The *third layer* is the deep Wumishan group (Jxw) dolomite, with a thickness of about 100 m (from 400 to 500 m), and it can be regarded as an impervious boundary.

Karst groundwater in Fangshan is divided into three major hydrogeological units with different characteristics: Beiling syncline hydrogeological unit, Dashihe anticline hydrogeological unit, and Xiayunling-Longmentai synclinorium hydrogeological unit, as shown in Fig. 3. The scope of sampling and analysis was extended beyond the

Table 3 Summary of stratigraphic units in the study area

System	Formations	Thickness (m)	Main rocks	Hydraulic properties
Quaternary (Q)	Late Pleistocene (Qp_3), Holocene (Qh)	10–20	Clay, sand and gravel	First aquifer: 0.5–20 m/day hydraulic conductivity, 500–1,000 m^3/day well yield
Cretaceous (K)	–	Not widely distributed	Sandstone, siltstone	–
Jurassic (J)	–	Not widely distributed	Clastic rocks	–
Permian (P)	Hongmiaoling (P_2h), Shihezi (P_1sh)	Not widely distributed	Sandstone, siltstone and shale	–
Carboniferous (C)	–	Not widely distributed	Sandstone, shale	–
Ordovician (O)	–	Not widely distributed	Limestone	–
Cambrian (∈)	–	Not widely distributed	Slate, limestone	–
Qingbaikou (Qn)	Jingeryu (Qbj), Xiamaling (Qbx)	Not widely distributed	Shale and slate	–
Jixian (Jx)	Tieling (Jxt), Hongshuizhuang (Jxh), Wumishan, (Jxw), Yangzhuang (Jxy)	300–500	Dolomite	Second aquifer and one aquitard: 0.5 ~ 50 m/day hydraulic conductivity, 2,000 m^3/day well yield
Changcheng (Ch)	Gaoyuzhuang (Chg)	Not widely distributed	Quartz sandstone and siliceous dolomite	–

study area to understand the relationship between the groundwater system of the study area and the regional geological structure, surface water and groundwater.

Beiling syncline hydrogeological unit

The aquifer is rich in water in the piedmont zone. The average groundwater depth is 20–30 m, and the average drawdown for wells in the area is 0.75–1.78 m. The flow of a single well at Caijawu is 668–1,334 m^3/day, and groundwater depth is about 10 m; when the well is pumped creating a drawdown of 2.65 m, the flow of the single well is 1,556 m^3/day. The village of Nanjiao has a high groundwater level, and the water level decreases from Beiling syncline in both outward directions. The water level in the north of this hydrogeological unit is significantly higher than that of the south. Groundwater level has a declining trend in Cijiawu, with a groundwater-level elevation of 93 m above sea level in 1980 and 83 m in 2010.

Springs are natural discharge points of karst aquifers. Wanfotang spring and Mapao spring are the two main springs located in this hydrogeological unit. Wanfotang spring is located to the north of Beiling syncline, and the spring discharge is mainly influenced by rainfall, with a significant fluctuation. Mapao spring is located to the south of the Beiling Syncline with a flow rate of 1,000–40,000 m^3/day. The Cambrian and Ordovician aquifer system is recharged; the recharged groundwater flows along the Beiling syncline to the piedmont, finally discharging at Mapao spring and Wanfotang spring.

The Ordovician limestone has a wide outcrop area near Dashi River at Cijiawu, and Dashi River leaks a large amount to groundwater. Karst groundwater in the Beiling syncline has a weak hydraulic connection with Dashi River; the water level of Dashi River is higher than that of the karst groundwater. This difference is obvious, for example, the water level of Dashi River has an elevation of 178 m (above sea level), but 100 m in a nearby cave, a difference of 78 m. The water level of Heilongguan spring has an elevation of 145 m, but 104 m in another cave, a difference of 41 m.

Dashihe anticline hydrogeological unit

In the south of Dashihe anticline hydrogeological unit, groundwater in the mountains is recharged by rainfall. Groundwater flows from west to east, turning to the south at the barrier of Xiamaling shale, and overflows to the ground surface, discharging at Heilongguan spring. Heilongguan spring is considered as the main source of Dashi River. The spring discharge is 1,556 m^3/day. The chemical characteristics indicate that although Heilongguan spring discharges from Tieling Formation (Jxt) strata, most of its recharge originates from groundwater in the Cambrian and Ordovician

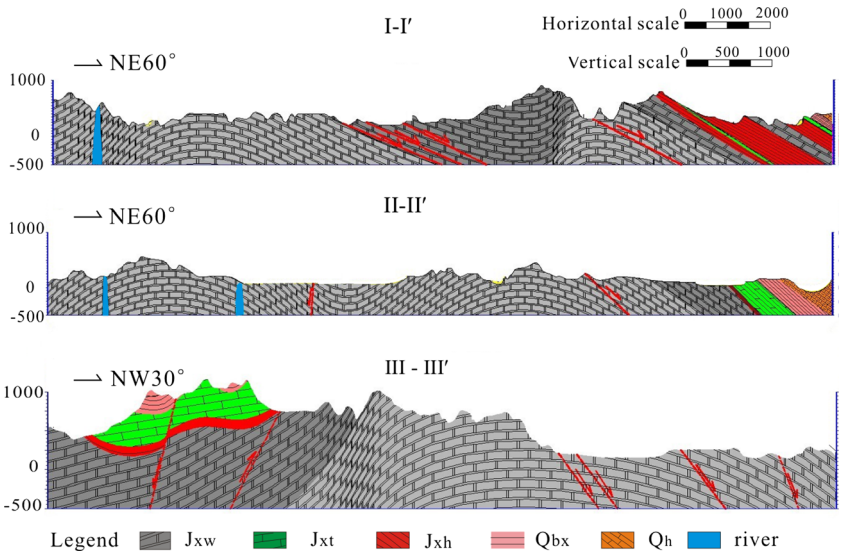

Fig. 2 Hydrogeological cross section of Fangshan, China

limestones. In the east of this hydrogeological unit, the strata is comprised of Cambrian limestone; groundwater flows from the north to the south, and forms Hebei spring to the north of Dashi River. Hebei spring flow is relatively stable, with a rate of 4,000–6,000 m^3/day. In the north of Dashihe anticline hydrogeological unit, the surface strata are comprised of Tieling Formation (Jxt) and Wumishan (Jxw) in the upstream section of Dashi River and exhibit the features of groundwater in dolomitic limestone.

Xiayunling-Longmentai synclinorium hydrogeological unit

The region is divided into two parts by the lamprophyre dyke at the village of Zhangfang-Ma'an. To the west of the dyke is a mountainous region, where groundwater is recharged by rainfall and flows to Juma Valley as the main source of the base flow. To the east of the dyke, the area includes mountains and piedmont; the Xiamaling shale is the unit's northern and eastern boundary, the lamprophyre dyke is the western boundary,

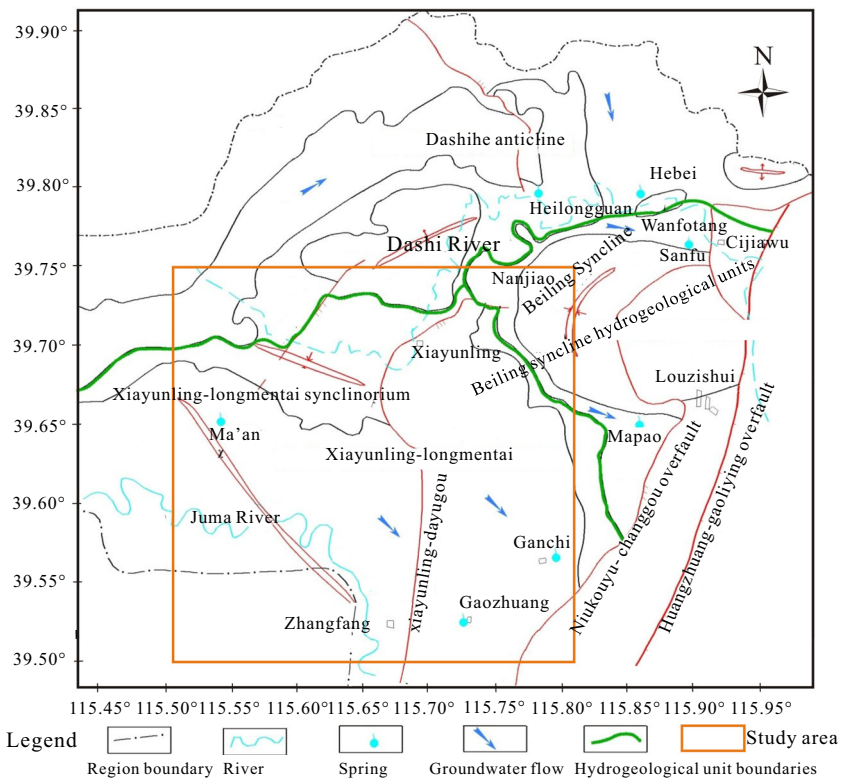

Fig. 3 The three hydrogeological units of the study area

and the Niukouyu-Changgou overfault is the southern boundary.

Characterization of the groundwater/surface-water interaction

Water chemistry

During long-term interaction with the surrounding environment, karst water develops its unique chemical characteristics. Water cycle information can be recorded to a certain extent, including water storage conditions, seepage flowpaths, recharge sources, and so on (McCoy et al. 2007; Nguyen et al. 2014; Martos-Rosillo and Moral 2015; Menning et al. 2015).

Water samples were taken from various sources, including surface water, Quaternary strata pore water, karst groundwater and springs. In the northwestern mountains, the concentration of total dissolved solids (TDS), hardness, Cl^-, and NO_3^- in bedrock groundwater are relatively low, but concentrations in groundwater in the piedmont region are higher. The hardness of Juma River is less than 250 mg/L, but the concentrations in samples from other places are greater than 250 mg/L, and the variation of TDS and hardness is similar to bedrock water. The chemical composition of the karst groundwater is similar to that of the surface water. According to the chemical quality data of karst groundwater and Juma River in 2006 (Table 4), it can be seen that the water-quality index parameters such as Ca^{2+}, Mg^{2+}, HCO_3^-, NO_3^-, TDS and hardness, have higher concentrations in the karst groundwater than in the river, but other index concentrations are basically similar. The water quality data for 2012 also show the same trend. The similarity of chemical composition for Juma River and the karst groundwater indicate that they have a close recharge–discharge relationship.

The TDS concentration of the karst water in the drainage area is lower than that in the surrounding area; this can be seen by comparing the results of groundwater analyses between Ganchi spring, Gaozhuang spring and the nearby groundwater. The TDS concentrations of Ganchi spring and Gaozhuang spring are significantly lower than those of bedrock groundwater samples from the northern spring group (Fig. 4). The two springs are located in the southeast of the study area, namely the groundwater discharge region. There is much dissolutional enlargement of fractures near the two springs, forming a good underground karst fracture channel and facilitating conditions for groundwater recharge-flow-discharge. The concentrations of HCO_3^-, Ca^{2+}, Mg^{2+} and other insoluble ions are higher here, but the TDS and hardness of groundwater are low.

According to the analytical data, the regional groundwater quality maintains stability, and the concentration of some components, such as hardness and TDS, are slightly higher than in the study area. The hardness of Ganchi and Gaozhuang spring waters in 1980 were about 248 and 220 mg/L, respectively. The hardness of Ganchi and Gaozhuang spring waters in 2000 were about 251 and 222 mg/L, and the hardness concentrations in 2012 were about 275 and 240 mg/L, respectively. The main reason for the increasing trend of groundwater TDS and hardness is that regional groundwater exploitation has increased dramatically since 2000, which has caused

Table 4 Water quality data of karst groundwater and Juma River samples

Water-quality index parameter	2006			2012		
	Surface water (mg/L)	Karst groundwater (mg/L)	Difference (mg/L)	Surface water (mg/L)	Karst groundwater (mg/L)	Difference (mg/L)
K^+	1.81	0.78	1.03	2.54	1.36	1.18
Na^+	7.15	8.02	−0.87	8.03	5.71	2.32
Ca^{2+}	39.1	70.7	−31.6	57.85	55.19	2.66
Mg^{2+}	20.7	31.6	−10.9	22.25	26.43	−4.18
Sr^{2+}	0.14	0.11	0.03	0.26	0.11	0.15
NH_4^+	0.03	0.02	0.01	0.13	0.12	0.01
HCO_3^-	167	327	−160	201.0	232.75	−31.75
Cl^-	8.2	11.3	−3.1	11.83	10.16	1.67
SO_4^{2-}	30.9	30.8	0.1	60.48	37.25	23.23
NO_3^-	2.3	24.1	−21.8	14.18	22.93	−8.75
F^-	0.2	0.35	−0.15	0.32	0.17	0.15
CO_2	0	6.6	−6.6	2.85	2.24	0.61
TDS	293	505	−212	394.00	407.75	−13.75
Hardness	183	307	−124	236.00	246.63	−10.63
pH	8.36	7.64	0.72	7.38	7.23	0.15

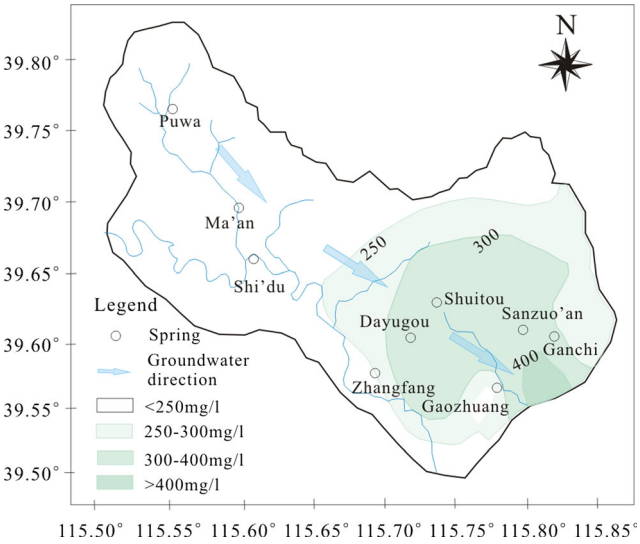

Fig. 4 The distribution of total dissolved solids (TDS) in the karst groundwater

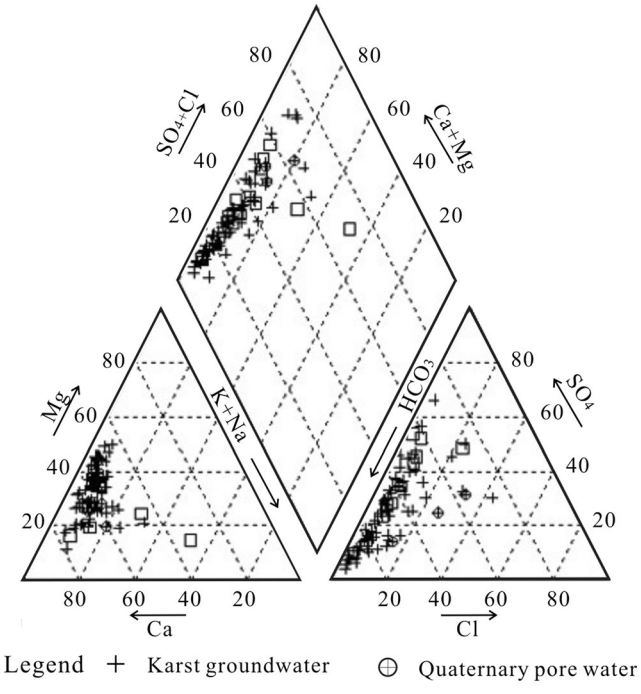

Fig. 5 Piper diagram for the *Quaternary pore water*, *karst groundwater*, and *surface water* samples

groundwater dynamic field and hydrogeochemical environment changes.

The concentrations of TDS, hardness, and chloride ions in the karst groundwater broadly increase from northwest to southeast, coincident with overall regional groundwater flow direction. The karst aquifer is mainly comprised of carbonate rocks in Wumishan, Tieling Formation, Ordovician, and Cambrian formations. The groundwater in dolomite rocks has a Mg^{2+}/Ca^{2+} ratio of between 0.611 and 0.87 with a F concentration of 0.05–0.31 mg/L, whilst Sr is generally less than 0.05 mg/L. The groundwater in the limestone rocks has a SO_4^{2-} content of 10–50 mg/L, a F concentration of less than 0.05 mg/L, and a Sr content of 0.28–1.68 mg/L. The dolomite of Wumishan formation (Jxw) has a high level of Mg and F, and the limestone of Ordovician and Cambrian rocks has high Sr and sulfate, which may explain the differences in groundwater chemical composition.

In order to identify the dominant water type of the study area all the samples were plotted in a Piper diagram (Fig. 5). All the water samples may be categorized as HCO_3–Ca·Mg and HCO_3·SO_4–Ca·Mg types. The Piper diagram also shows that most samples contain Ca^{2+}+ Mg^{2+} as the predominant cations, the concentration of Ca^{2+} is obviously higher than that of Mg^{2+}, and the concentration of K^++ Na^+ is low. Besides, HCO_3^- and SO_4^{2-} are the dominant anions in the water samples, and the concentration of Cl^- is low. Some surface water samples show higher K^++ Na^+ than groundwater, but overall there is a similarity with the groundwater composition. In general, the water chemistry type of the karst groundwater shows consistency with that of Quaternary pore water and surface water, and the results imply that they are hydrochemically similar and related, and probably have a close transformation relationship and hydraulic connection.

Isotopes

The stable isotopes of oxygen-18 (^{18}O) and deuterium (^2H or δD) can help to identify potential flow paths from rainfall infiltration to groundwater, and to study the interaction of surface water and groundwater as conservative tracers (Lambán et al. 2015; Martinez et al. 2015; Lee et al. 2016). Twenty-nine groundwater samples were collected for isotope analysis, and the sampling positions are shown in Fig. 1.

The groundwater samples present an isotopic composition ranging from −10.20 to −8.75‰ (average −9.34‰) for $\delta^{18}O$ and from −69.6 to −62.2‰ (average −65.48‰) for δD. In Fig. 6, the stable isotope data are shown together with the local meteoric water line (LMWL) for rainwater (Song et al. 2007; Wen et al. 2010), clearly showing that all samples plot close to the LMWL, thus indicating that the groundwater is recharged by the local rainfall. From the northwest and northeast mountain regions to the piedmont zone in the southeast, $\delta^{18}O$ and δD of karst water generally showed an increasing trend. The LMWL is given by $\delta D = 7.3\delta^{18}O + 9.7$; most of groundwater data points fall below this line, and one equilibrium line for groundwater is given by $\delta D = 5.1\delta^{18}O - 18.2$ (Fig. 6), which may indicate that evaporation of falling raindrops has happened before groundwater recharge has taken place. The values of $\delta^{18}O$ will change under the effect of average global elevation (0.15–0.50‰/100 m), thus groundwater of different regions receives recharge from different rainwater sources. If the values of $\delta^{18}O$ and δD are relatively low, the elevation of

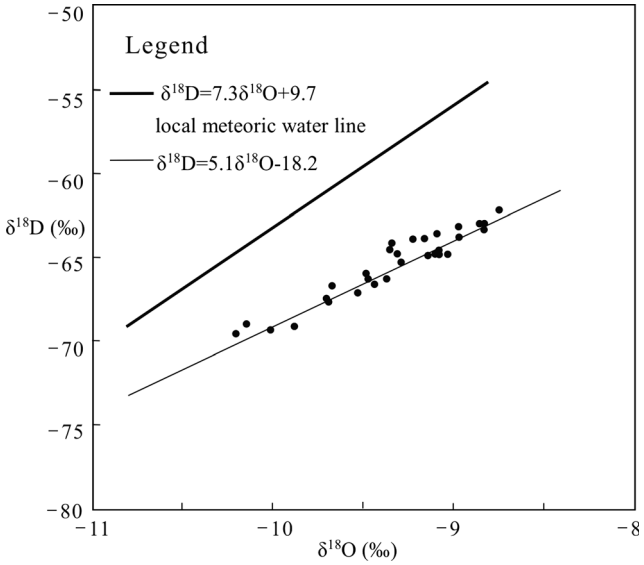

Fig. 6 Deuterium vs oxygen-18 for selected sampling points

the groundwater source region is high, and if the values of $\delta^{18}O$ and δD are high, the elevation of the groundwater source region is low. For this study, the deuterium excess value, gradually decreasing from the northwest to southeast, is in agreement with the observed direction of groundwater flow.

Twenty-nine samples of groundwater and four samples of surface water were also collected for the analysis of tritium (^3H), a radioactive isotope. Groundwater sample locations were the same as the locations used for $\delta^{18}O$ and δD analysis; the four samples of surface water for tritium (^3H) analysis are also shown in Fig. 1. The surface-water samples were taken from Dashi River and Juma River, and the groundwater samples were taken from Quaternary groundwater and karst water. The concentrations of ^3H in Dashi River and Juma River are 18.4 and 21.7 TU, respectively, which is close to the value of rainfall. The concentration of ^3H in the karst groundwater ranges from 3.2 to 26.3 TU; tritium concentration ranges from 16 to 22 TU for most groundwater samples, but ranges from 13.2 to 16.1 TU for the samples of Ma'an spring and Shuitou spring, and ranges from 3.2 to 13.5 TU for the southeast of the study area.

The spatial variation characteristics of ^3H concentration can reflect the relationship for the karst groundwater of different regions. The concentration of ^3H is about 16–24 TU in groundwater to the north of Juma River, and 12.2 TU to the south of Juma River, which implies that a channel from the north to the south exists in the bedrock aquifer. The concentration of ^3H is about 12.7–15.1 TU for Gaozhuang spring, but about 19.1–22 TU for Huinanzhuang spring to the south of Gaozhuang spring, which shows that there is an aquitard comprised of interbedded phyllite, marble and sandstone to the south of Gaozhuang spring. The concentration for ^3H in the southeast of the study area is low. This shows that the karst groundwater in this area has been in circulation for a long distance and at large depth, and the main recharge source is the rainfall infiltration in the northern mountainous area.

Groundwater level

Zhangfang water source was developed to ease the pressure of urban water supply in Beijing, and the water supply capacity at Zhangfang has reached 2×10^5 m^3/day. The groundwater exploitation of Zhangfang water source plays a pivotal role in the drainage of the karst groundwater system in the Fangshan region.

Groundwater level, groundwater exploitation and rainfall time-series data over eight hydrological years have been used for identifying their relationship and the patterns of exploitation since 2006. The monitoring well named W216 was selected on the basis of the most continuous dataset. It shows a smooth and seasonal change between recharge and recession periods with an annual water-level variation of 8–10 m, and the lag responses to rainfall events have been determined. Groundwater level is highest in the rainy season (August and September), and the lowest level is in the dry season (May and June).

Cross-correlation analysis was used to investigate the relationship between groundwater level, groundwater exploitation and rainfall (Panagopoulos and Lambrakis 2006). Figure 7 presents the cross-correlation functions (CCF) results; the vertical coordinates represent the correlation between groundwater level and rainfall (or groundwater exploitation). The correlation coefficient is greater than zero if it is positively correlated with groundwater level, but the correlation coefficient is less than zero if it is negatively correlated with groundwater level, and the horizontal coordinates represent the response time of the groundwater level in relation to different rainfall or groundwater exploitation events. The time when the absolute value of the correlation coefficient reaches the maximum represents the lag time. It can be seen that the absolute value of correlation coefficient between groundwater level and rainfall reaches the maximum at a lag time of 2 months, and the absolute value of correlation coefficient

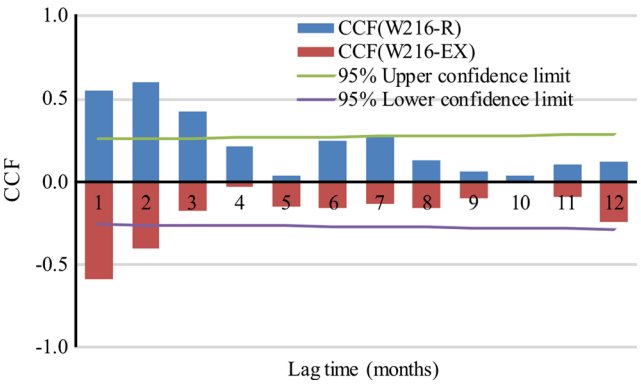

Fig. 7 Cross-correlation functions (*CCF*) between groundwater level at well *W216*, and groundwater exploitation (*EX*) and rainfall (*R*)

between groundwater level and groundwater exploitation reaches the maximum at a lag time of 1 month.

Rainfall infiltration is the main recharge source of the groundwater, and it has a significant effect on the groundwater level (Allocca et al. 2015; Cai and Ofterdinger 2016). The longer response time (2 months) for a peak value of CCF between rainfall and groundwater level may indicate that the groundwater infiltration process is complex and influenced by the vadose zone and shallow bedrock. When the exploitation is large, and groundwater level decreases sharply, but when the exploitation is stopped, groundwater level can recover to a certain extent.

Spectral analysis is complementary to correlation analysis. The spectral density functions (SDF) of groundwater level, groundwater exploitation and rainfall are presented in Fig. 8. The peaks of the SDF at a frequency of 0.16 month^{-1} were found both in groundwater level and rainfall data; the period equals to the reciprocal of frequency, which means that groundwater level and rainfall data have the same period of 6 months. This is consistent with the cross-correlation analysis indicating that groundwater level has a close correlation with rainfall and groundwater exploitation under the appropriate conditions of rainfall infiltration and frequent human activities. The aquifer is comprised of dolomitic limestone in the northwest part of the study area and most of the area is directly exposed at the ground surface and is highly fractured, so the conditions for rainfall infiltration are good.

A multiple non-linear regression (MNR) model was also constructed to reflect the relationship between groundwater level depth and impact factors (groundwater exploitation and rainfall). The MNR results are shown in Fig. 9 with the 3D plots of groundwater level depth versus groundwater exploitation and rainfall. The MNR model can be written as:

$$y = -0.79 - 0.005\tilde{n}_1 - 0.076\tilde{n}_2 - 0.00027\tilde{n}_1^2 - 0.00003\tilde{n}_2^2 + 0.0001\tilde{n}_1\tilde{n}_2 \quad (1)$$

where y, x_1, x_2, are groundwater level depth (m), rainfall (mm), and groundwater exploitation (10^4 m^3/day), respectively.

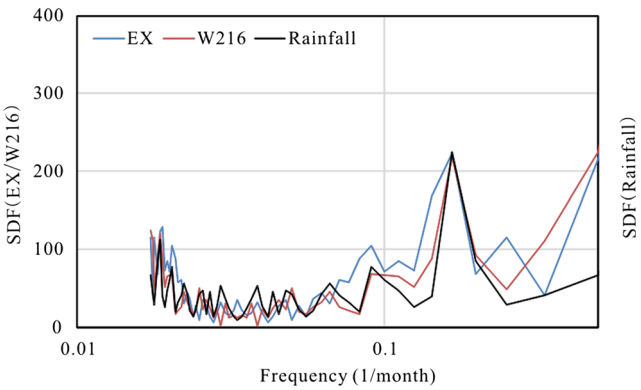

Fig. 8 Spectral density functions (*SDF*) of groundwater level at well *W216* versus groundwater exploitation (*EX*) and rainfall

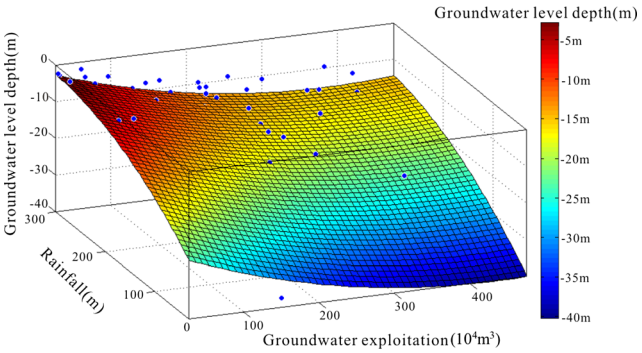

Fig. 9 Three-dimensional plot of groundwater level against groundwater exploitation and rainfall

The statistical term correlation coefficient (R^2) was selected to evaluate the fitting ability of the MLR model. R^2 equals 0.75, which means the MNR model can reflect the relationship between groundwater level and rainfall and groundwater exploitation. The coefficients also confirm the direct relationships between groundwater level and rainfall, and there is a remarkable nonlinear correlativity between groundwater level and groundwater exploitation. On increasing rainfall, groundwater level will increase, but groundwater level will decrease with increasing groundwater exploitation. The results indicate groundwater level will be negatively correlated with groundwater exploitation, and positively correlated with rainfall.

Juma River is the only perennial river in the study area, and has a close interaction with groundwater. According to water-level investigations, Juma River receives recharge from groundwater above Zhangfang station with the exchange rate of about 132×10^4 m^3 in the form of springs and base flow, such as Ma'an spring. However, Juma River discharges to groundwater below Zhangfang station with the exchange rate of about 130×10^4 m^3, where the stream gradient is large and the groundwater depth is big. Here, the groundwater (of mixed groundwater and surface-water origin) becomes the main supply source for Huinanzhuang.

The amount and area of agricultural irrigation in the study area are both small. In most areas, agricultural irrigation mainly occurs in the spring and autumn, and the irrigation is sourced from groundwater and Juma River. Whilst well irrigation leads to falling groundwater levels, river irrigation leads to rising groundwater levels.

The heaviest daily rainfall in Beijing since 1951 occurred on 21 July 2012, known as the "7.21" event, when the rainfall continued for nearly 16 h. Whereas the average rainfall of Beijing is 170 mm during this one rainfall period of 16 h, the maximum value of 460 mm was reached in Fangshan District (Xie et al. 2016). This event occurred during a period of falling groundwater levels. The groundwater responded rapidly to individual rainfall events on 21 July 2012, rising at three different sites by 2, 8, and 11 m, respectively. Groundwater level has a lag of 5–10 days behind rainfall in

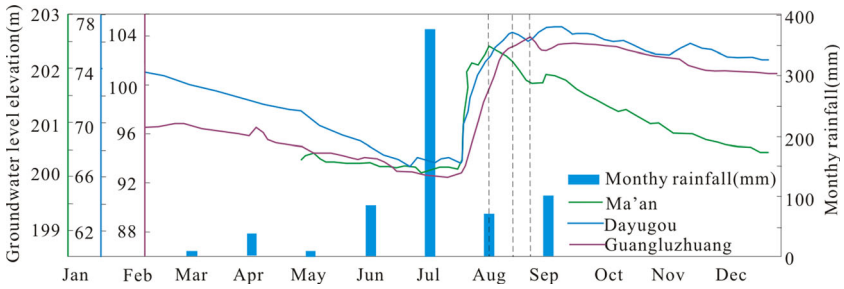

Fig. 10 Groundwater level and rainfall in typical monitoring wells

the mountainous region (such as the villages of Ma'an, Dayugou, Guangluzhuang, Fig. 10). The results suggest groundwater is closely correlated with rainfall.

Discussion of the results

Water chemistry data show that the groundwater flow system has unified recharge and discharge conditions, and karst groundwater and Quaternary pore water quality are consistent with that of surface water. However, the salinity of the karst water in the spring discharge regions is lower than the surrounding regions, so there may be a number of relatively independent smaller-scale hydrogeological units.

The karst groundwater has a similar characteristic in terms of the stable isotopes of $\delta^{18}O$ and δD to that of rainfall. Karst features develop readily at the ground surface in the mountainous region, so conditions for vertical infiltration are suitable, and groundwater is quickly recharged by rainfall. In addition, the spatial distribution of the concentration of ^{3}H also shows that there is a distal groundwater source from northern mountainous areas, a distance of about 10 km away. Groundwater flow has stratified characteristics; the groundwater flow paths are closely related to surface water, that is, the interaction of surface water and groundwater is very strong.

The discovery of stratified groundwater flow can contribute to the understanding of pathways of GW–SW interaction, which reflects the following:

1. *Geological structure*. There are fold and thrust structures, forming the deep fracture zone. Water yield is not good above 100-m depth in the strata in the Baidai area, but the strata are fractured and water-saturated below 100-m depth. The Sanzuo'an anticline has obvious resistance to groundwater flow. If the Gaozhuang springs catchment was delimited by the Sanzuo'an anticline, the springs would not reach the current discharge volume, so the baseflow catchment of Gaozhuang springs must reach to the north of Sanzuo'an anticline, and groundwater can discharge to Gaozhuang spring in the form of a deep-layer flowpath that bypasses the anticline (Fig. 1).
2. *The concentration of cations in the groundwater recharge area and the discharge area of springs is low, but that of the area which is located between the recharge area and the discharge area is high*. This phenomenon can be explained by stratified groundwater flow, that is, groundwater originating in the recharge area flows via deep-layer flowpaths and reaches the discharge area in the piedmont plain bypassing the shallow layers (Fig. 4).
3. *Springs*. The average discharge at Gaozhuang springs is $1{,}700 \times 10^4$ m^3/year, and over the same period (2004–2014) the average annual rainfall is 530 mm; the surface watershed area is 42 km^2 and the permeability is 0.35 m^2, so the infiltration recharge is 780×10^4 m^3/year, which is less than the spring discharge. Thus, the catchment of the spring group is greater than the surface watershed area.

The cross-correlation analysis reveals that groundwater level is mainly affected by rainfall and groundwater exploitation with a more rapid response to groundwater exploitation than rainfall (Fig. 7). For rainfall, the cross-correlation functions show a good correlation (peak CCF 0.60) between rainfall and groundwater level for two wells within a time delay of 2 months, and a good correlation (peak CCF 0.57) was also found between groundwater exploitation and groundwater level with a time lag of 1 month. The spectral analysis result also reveals that groundwater level, groundwater exploitation and rainfall respond to each other within the same significant periods, which indicates their possible internal relationship. Furthermore, the MNR model indicates that groundwater levels are negatively correlated with groundwater exploitation, and positively correlated with rainfall. It was also found that there is a direct relationship between groundwater exploitation, rainfall and groundwater level. This fact is in agreement with the aforementioned studies reported by cross-correlation functions and spectral analysis. Some other evidence also suggests groundwater is in close correlated to rainfall and surface water.

Conclusion

The study area, Fangshan in northern China, is known as a typical karst landscape, which is mainly composed of sedimentary and metamorphic rock; the Wumishan group (Jxw) dolomite is exposed over the entire area. The aquifer system consists of three layers: Quaternary aquifer, karst aquifer with

developed fractures, and karst aquifer with undeveloped fractures. The karst groundwater system can be divided into three major hydrogeological units with different characteristics, named in association with Beiling syncline, Dashihe anticline, and Xiayunling-longmentai synclinorium. The main karst aquifer is comprised of many fractures, leading to water resources that are comparatively abundant.

The interaction of groundwater and surface water is strong in the karst aquifer. Hydrochemical, isotope and groundwater level data analysis were conducted to characterize the interaction of groundwater and surface water. Water chemistry data show that chemistry type and the concentrations of parameters in the karst groundwater show consistency with that of the surface water. Stable isotope ratios of all samples show proximity to the local meteoric water line. ^{3}H data show the range 18.4–21.7 TU in surface water and the range 16.1–22.3 TU in groundwater, which are both close to the background value of ^{3}H in the rainfall. Stable and radio-isotopes also confirm karst groundwater is recharged by rainfall.

Cross-correlation analysis and spectral analysis were used to investigate the relationship between groundwater level and groundwater exploitation vs. rainfall. The cross-correlation analysis showed that groundwater level is mainly affected by rainfall and groundwater exploitation, with more rapid response to groundwater exploitation than rainfall. A similar periodic response is evident with regard to the groundwater level and groundwater exploitation. Furthermore, MNR modelling indicates that groundwater levels will be negatively correlated with groundwater exploitation, and positively correlated with rainfall. The results revealed that groundwater level has a strong correlation with rainfall. These findings are important in that they are indicative of a close hydraulic connection and interaction between surface water and groundwater in the study area. Characterization of GW–SW interactions can greatly assist with a better understanding of hydrological connectivity between surface water and groundwater, and it can provide more information to modelers and engineers for the development of conceptual and numerical models, which will improve the accuracy of the models without the repeated consideration of the exchange fluxes between groundwater and surface water in the calculation process. A good understanding of hydrogeological characteristics and GW–SW interaction provides a reliable basis for managing water resources, and it also has important practical significance for the rational utilization of karst water and relieve the supply–demand contradictions.

Acknowledgments The research was financially supported by the National Natural Science Foundation of China (51459003) and the Project of Karst Groundwater Resources Exploration and Assessment in Beijing (BJYRS-ZT-01), and the Special Fund for Public Welfare Industry of the Ministry of Water Resources in China (No. 201501028). Comments and suggestions from anonymous reviewers, the associate editor, and the editor are greatly appreciated.

References

Allocca V, De Vita P, Manna F, Nimmo JR (2015) Groundwater recharge assessment at local and episodic scale in a soil mantled perched karst aquifer in southern Italy. J Hydrol 529:843–853

Banks EW, Simmons CT, Love AJ, Cranswick R, Werner AD, Bestland EA, Wood M, Wilson T (2009) Fractured bedrock and saprolite hydrogeologic controls on groundwater/surface-water interaction: a conceptual model (Australia). Hydrogeol J 17(8):1969–1989

Brunner P, Simmons CT, Cook PG, Therrien R (2010) Modeling surface water-groundwater interaction with MODFLOW: some considerations. Ground Water 48(2):174–180

Bureau of Geology and Mineral Resources of Beijing Municipality (BGMRBM) (1991) Regional Geology of Beijing Municipality. Geological Publishing House, Beijing, pp 8–34

Cai Z, Ofterdinger U (2016) Analysis of groundwater-level response to rainfall and estimation of annual recharge in fractured hard rock aquifers, NW Ireland. J Hydrol 535:71–84

Charlier JB, Bertrand C, Mudry J (2012) Conceptual hydrogeological model of flow and transport of dissolved organic carbon in a small Jura karst system. J Hydrol 460:52–64

Dafny E, Burg A, Gvirtzman H (2010) Effects of Karst and geological structure on groundwater flow: the case of Yarqon-Taninim Aquifer, Israel. J Hydrol 389(3):260–275

Daly D, Dassargues A, Drew D, Dunne S, Goldscheider N, Neale S, Popescu IC, Zwahlen F (2002) Main concepts of the "European approach" to karst-groundwater-vulnerability assessment and mapping. Hydrogeol J 10(2):340–345

Devito KJ, Hill AR, Roulet N (1996) Groundwater–surface water interactions in headwater forested wetlands of the Canadian Shield. J Hydrol 181(1):127–147

Doglioni A, Simeone V (2014) Data-driven modeling of the dynamic response of a large deep karst aquifer. Proc Eng 89:1254–1259

Eris E, Wittenberg H (2015) Estimation of baseflow and water transfer in karst catchments in Mediterranean Turkey by nonlinear recession analysis. J Hydrol 530:500–507

Gill LW, Naughton O, Johnston PM, Basu B, Ghosh B (2013) Characterisation of hydrogeological connections in a lowland karst network using time series analysis of water levels in ephemeral groundwater-fed lakes (turloughs). J Hydrol 499:289–302

Green RT, Bertetti FP, Miller MS (2014) Focused groundwater flow in a carbonate aquifer in a semi-arid environment. J Hydrol 517:284–297

Jukić D, Denić-Jukić V (2015) Investigating relationships between rainfall and karst-spring discharge by higher-order partial correlation functions. J Hydrol 530:24–36

Kalbus E, Reinstorf F, Schirmer M (2006) Measuring methods for groundwater–surface water interactions: a review. Hydrol Earth Syst Sci 10(6):873–887

Kumar M, Ramanathan AL, Keshari AK (2009) Understanding the extent of interactions between groundwater and surface water through major ion chemistry and multivariate statistical techniques. Hydrol Proc 23(2):297–310

Lambán LJ, Jódar J, Custodio E, Soler A, Sapriza G, Soto R (2015) Isotopic and hydrogeochemical characterization of high-altitude karst aquifers in complex geological settings: the Ordesa and Monte Perdido National Park (northern Spain) case study. Sci Total Environ 506:466–479

Lee S, Currell M, Cendón DI (2016) Marine water from mid-Holocene sea level highstand trapped in a coastal aquifer: evidence from groundwater isotopes, and environmental significance. Sci Total Environ 544:995–1007

Martinez JL, Raiber M, Cox ME (2015) Assessment of groundwater–surface water interaction using long-term hydrochemical data and

isotope hydrology: headwaters of the Condamine River, Southeast Queensland, Australia. Sci Total Environ 536:499–516

Martos-Rosillo S, Moral F (2015) Hydrochemical changes due to intensive use of groundwater in the carbonate aquifers of Sierra de Estepa (Seville, southern Spain). J Hydrol 528:249–263

McCoy CA, Corbett DR, Cable JE, Spruill RK (2007) Hydrogeological characterization of southeast coastal plain aquifers and groundwater discharge to Onslow Bay, North Carolina (USA). J Hydrol 339(3): 159–171

Menning DM, Wynn JG, Garey JR (2015) Karst estuaries are governed by interactions between inland hydrological conditions and sea level. J Hydrol 527:718–733

Naughton O, Johnston PM, Gill LW (2012) Groundwater flooding in Irish karst: the hydrological characterisation of ephemeral lakes (turloughs). J Hydrol 470:82–97

Nguyen TT, Kawamura A, Tong TN, Nakagawa N, Amaguchi H, Gilbuena R (2014) Hydrogeochemical characteristics of groundwater from the two main aquifers in the Red River Delta, Vietnam. J Asian Earth Sci 93:180–192

Owor M, Taylor R, Mukwaya C, Tindimugaya C (2011) Groundwater/surface-water interactions on deeply weathered surfaces of low relief: evidence from lakes Victoria and Kyoga, Uganda. Hydrogeol J 19(7):1403–1420

Oxtobee JP, Novakowski K (2002) A field investigation of groundwater/surface water interaction in a fractured bedrock environment. J Hydrol 269(3):169–193

Panagopoulos G, Lambrakis N (2006) The contribution of time series analysis to the study of the hydrodynamic characteristics of the karst systems: application on two typical karst aquifers of Greece (Trifilia, Almyros Crete). J Hydrol 329(3):368–376

Rodgers P, Soulsby C, Petry J, Malcolm I, Gibbins C, Dunn S (2004) Groundwater–surface water interactions in a braided river: a tracer-based assessment. Hydrol Proc 18(7):1315–1332

Rugel K, Golladay SW, Jackson CR, Rasmussen TC (2016) Delineating groundwater/surface water interaction in a karst watershed: lower Flint River Basin, southwestern Georgia, USA. J Hydrol Region Stud 5:1–19

Schmidt S, Geyer T, Guttman J, Marei A, Ries F, Sauter M (2014) Characterisation and modelling of conduit restricted karst aquifers: example of the Auja spring, Jordan Valley. J Hydrol 511:750–763

Scibek J, Allen DM, Cannon AJ, Whitfield PH (2007) Groundwater–surface water interaction under scenarios of climate change using a high-resolution transient groundwater model. J Hydrol 333(2):165–181

Song XF, Li FD, Yu JJ, Tang CY, Yang C, Liu XC, Sakura Y, Kondoh A (2007) Characteristics of groundwater cycle using deuterium, oxygen-18 and hydrochemistry in Chaobai River Basin. Geogr Res 26(1):11–21

Sun J, Tang C, Wu P, Strosnider WH, Han Z (2013) Hydrogeochemical characteristics of streams with and without acid mine drainage impacts: a paired catchment study in karst geology, SW China. J Hydrol 504:115–124

Sun F, Yang Z, Huang Z (2014) Challenges and solutions of urban hydrology in Beijing. Water Resour Manag 28(11):3377–3389

Wang W, Meng X, Peng Z, Chen QF, Liu N (2015) Increasing background seismicity and dynamic triggering behaviors with nearby mining activities around Fangshan Pluton in Beijing, China. J Geophys Res 120(8):5624–5638

Ward AS, Gooseff MN, Singha K (2010) Characterizing hyporheic transport processes: interpretation of electrical geophysical data in coupled stream-hyporheic zone systems during solute tracer studies. Adv Water Resour 33(11):1320–1330

Wei WS (2008) Fifty years of Beijing geological work. China Earth Press , Beijing, pp 39–77

Wei JH, Chu HB, Wang R, Jiang Y (2015) Numerical simulation of karst groundwater system for discharge prediction and protection design of spring in Fangshan District, Beijing. J Groundwater Sci Eng 3(4): 316–330

Wen XF, Zhang SC, Sun XM, Yu GR, Lee X (2010) Water vapor and precipitation isotope ratios in Beijing, China. J Geophys Res 115(D1):1–10

Xie Y, Xing J, Shi J, Dou Y, Lei Y (2016) Impacts of radiance data assimilation on the Beijing 7.21 heavy rainfall. Atmos Res 169: 318–330

Xu H, Song Y, Ye K, Zhang J, Wang H (2012a) Petrogenesis of mafic dykes and high-Mg adakitic enclaves in the Late Mesozoic Fangshan low-Mg adakitic pluton, North China Craton. J Asian Earth Sci 54:143–161

Xu L, Xin BD, Xu YL, Guo GX, Lu HY, Ji YQ, Shen YY (2012b) Assessment of over exploitation of groundwater in the Fangshan Plain of Beijing. Water Sci Technol 10(4):112–115

Yang N, Yuan QL, Sun L, Zhou J, Li SJ (2014a) Assessment on the vulnerability of Fangshan karst groundwater in Beijing based on European model. Adv Mat Res 838:1772–1775

Yang Z, Zhou Y, Wenninger J, Uhlenbrook S (2014b) A multi-method approach to quantify groundwater/surface water-interactions in the semi-arid Hailiutu River basin, northwest China. Hydrogeol J 22(3): 527–541

Yao Y, Huang X, Liu J, Zheng C, He X, Liu C (2015) Spatiotemporal variation of river temperature as a predictor of groundwater/surface-water interactions in an arid watershed in China. Hydrogeol J 23(5): 999–1007

Zeng C, Liu Z, Yang J, Yang R (2015) A groundwater conceptual model and karst-related carbon sink for a glacierized alpine karst aquifer, Southwestern China. J Hydrol 529:120–133

Zhan C, Zhang Y, Xia J (2012) Hydrologic response to climate variability and human activities in the Chao River catchment near Beijing. Water Int 37(5):585–597

Zhang Y, Smith JA, Luo L, Wang Z, Baeck ML (2014) Urbanization and rainfall variability in the Beijing metropolitan region. J Hydrometeorol 15(6):2219–2235